Available online at www.sciencedirect.com
SCIENCE DIRECT
Coastal Engineering 53 (2006) 141 – 147
Coastal Engineering
An International Journal for Coastal, Harbour and Offshore Engineers
www.elsevier.com/locate/coastaleng

Numerical modeling of water waves with the SPH method

R.A. Dalrymple *, B.D. Rogers [1]

Department of Civil Engineering, Johns Hopkins University, 3400 N Charles Street, Baltimore, MD 21218, USA

Available online 7 December 2005

As Prof. Jurjen Battjes has long worked in the area of waves and has inspired the authors throughout their careers, we dedicate this paper to him.

Abstract

Smoothed Particle Hydrodynamics (SPH) is a relatively new method for examining the propagation of highly nonlinear and breaking waves. At Johns Hopkins University, we have been working since 2000 to develop an engineering tool using this technique. However, there have been some difficulties in taking the model from examples using a small number of particles to more elaborate and better resolved cases.

Several improvements that we have implemented are presented here to handle turbulence, the fluid viscosity and density, and a different time-stepping algorithm is used. The final model is shown to be able to model breaking waves on beaches in two and three dimensions, green water overtopping of decks, and wave–structure interaction.

Keywords: Numerical methods; Hydrodynamics; Waves; Turbulence; SPH

1. Introduction

There are a variety of modern numerical methods to describe near breaking and breaking waves, including boundary element methods (e.g., Grilli et al., 2000), and methods taken from computational fluid dynamics: Direct Numerical Simulation (DNS; Lin and Liu, 1998; Chen et al., 1999), Reynolds Averaged Navier Stokes (RANS), and Large Eddy Simulation (LES) models (e.g. Wu (2004)). More recently the Smoothed Particle Hydrodynamics (SPH) method has been adapted from astrophysics into a number of fields, including free surface flows (Monaghan, 1994; Monaghan and Kos, 1999).

SPH offers a variety of advantages for fluid modeling, particularly those with a free surface. The Lagrangian method is meshfree; the equivalents of mesh points are the fluid particles moving with the flow. The free surface requires no special approaches, such as the volume-of-fluid method or a Lagrangian surface tracking. Furthermore, the method can treat rotational flows with vorticity and turbulence.

This paper presents a state-of-the-art review of improvements and enhancements we have made to the basic SPH methodology at The Johns Hopkins University (JHU). In the second part of the paper, we present examples of some of the basic applications that we have attempted to date.

2. Methodology

Smoothed Particle Hydrodynamics (SPH) can be considered as computing the trajectories of particles of fluid, which interact according to the Navier–Stokes equations. An alternative view is that the fluid domain is represented by nodal points that are scattered in space with no definable grid structure and move with the fluid. Each of these nodal points carry scalar information, density, pressure, velocity components, etc. To find the value of a particular quantity at an arbitrary point, **x**, we apply an interpolation:

$$f(\mathbf{x}) = \sum_j f_j W(\mathbf{x} - \mathbf{x}_j) V_j \qquad (1)$$

Here f_j is the value of f associated with particle j, located at $\mathbf{x}_j$, $W(\mathbf{x}-\mathbf{x}_j)$ represents a weighting of the contribution of particle j to the value of $f(\mathbf{x})$ at position $\mathbf{x}$, and V_j is the volume of particle j, defined as the mass, m_j, divided by the density of the particle, ρ_j. The weighting function, $W(\mathbf{x}-\mathbf{x}_j)$, is called the kernel and varies with distance from **x**. Its form is an approximation to a delta function. There are a variety of possible weighting functions (see Liu and Liu, 2003), we

* Corresponding author.
E-mail addresses: rad@jhu.edu (R.A. Dalrymple), bdr@jhu.edu (B.D. Rogers).
[1] Present address: Federal Technical Institute of Lausanne, Switzerland.

0378-3839/$ - see front matter © 2005 Elsevier B.V. All rights reserved.
doi:10.1016/j.coastaleng.2005.10.004

use a quadratic kernel, which has no inflection in its derivative:

$$W_{ij} = W(\mathbf{x}_i - \mathbf{x}_j) = \alpha_N (q^2/4 - q - 1) \qquad \text{where } q = r_{ij}/h \tag{2}$$

and $\alpha_N = \frac{3}{2\pi h^2}$ for 2-D, $\alpha_N = \frac{15}{16\pi h^3}$ for 3-D, $r_{ij} = |\mathbf{x} - \mathbf{x}_j|$ and the factor h is the smoothing length of the kernel.

While the summation in Eq. (1) implies that there is an interaction between all of the particles in the fluid domain, in practice the influence of the kernel is restricted to a radial distance of order $2h$. Only particles within this distance of point $\mathbf{x}$ contribute to the summation. In terms of modeling, techniques such as nearest neighbor lists are used to keep track of the particle positions, so that the summation above is truncated to only include the neighbors of the point of interest. This leads to immense time savings and is essential to the methodology.

The conservation of mass and the conservation of momentum are written in particle form (Monaghan, 1992). These are

$$\frac{d\rho_i}{dt} = \sum_j m_j (\mathbf{u}_i - \mathbf{u}_j) \cdot \nabla_i W_{ij} \tag{3}$$

$$\frac{d\mathbf{u}_i}{dt} = -\sum_j m_j \left(\frac{P_i}{\rho_i^2} + \frac{P_j}{\rho_j^2} + \Pi_{ij} \right) \nabla_i W_{ij} + \mathbf{g} \tag{4}$$

where $\mathbf{u}_j$ is the velocity of the particle, P_j is the pressure at the particle, m_j is the mass of particle j, $\nabla_i W_{ij} = \nabla_i W(\mathbf{x}_i - \mathbf{x}_j) = \frac{\partial W_{ij}}{\partial x_i} \boldsymbol{i} + \frac{\partial W_{ij}}{\partial y_i} \boldsymbol{j}$ (with $\boldsymbol{i}$ and $\boldsymbol{j}$ being unit vectors in coordinate directions and the first subscript i after nabla referring to the derivative of W_{ij} with respect to the coordinates of the particle i). Π_{ij} is an empirical term representing the effects of viscosity (Monaghan, 1992):

$$\Pi_{ij} = -\frac{\alpha \mu_{ij} \bar{c}_{ij}}{\bar{\rho}_{ij}}, \tag{5}$$

where α is an empirical coefficient (usually taken as 0.01–0.1), $\bar{c}_{ij} = (c_i + c_j)/2$, $\bar{\rho}_{ij} = (\rho_i + \rho_j)/2$ and $\mu_{ij} = h(\mathbf{u}_i - \mathbf{u}_j) \cdot (\mathbf{x}_i - \mathbf{x}_j)/(r_{ij}^2 + 0.01h^2)$.

In addition, particles are moved with the following equation:

$$\frac{d\mathbf{r}_i}{dt} = \mathbf{u}_i + \epsilon \sum_j m_j \left(\frac{\mathbf{u}_i - \mathbf{u}_j}{\bar{\rho}_i} \right) W_{ij}. \tag{6}$$

The last term, including the parameter $\epsilon \approx 0.5$, is the so-called XSPH correction of Monaghan (1989), which ensures that neighboring particles move with approximately the same velocity. This prevents particles with different velocities occupying nearly the same location.

The last equation needed is the equation of state that relates the pressure in the fluid to the local density.

$$P = B\left[\left(\frac{\rho}{\rho_0} \right)^{\gamma} - 1 \right]. \tag{7}$$

The factor γ is taken as 7. This equation implies that the fluid is compressible, and that there is a speed of sound ($C_s^2 = \partial P/\partial \rho$), which we set (by changing the value of B) to be approximately ten times the maximum wave velocity to be modeled. The correct sound speed is not used as it would require far smaller time steps for stability of the numerical model. Since the Mach number, $M = u_{max}/c = 0.1$, and compressibility effects are $O(M^2)$, the changes in fluid density are 1% or less.

The equation of state provides an advantage of giving a direct relationship between density and pressure, rather than having to solve, in the incompressible case, a Poisson equation for pressure (as in the MPS methodology, Koshizuka et al., 1998).

The above equations are solved numerically by time-stepping. We currently use the Verlet (1967) algorithm that provides a second-order accurate single step method, rather than a conventional two-step method (e.g. Monaghan, 1992). We have found the Verlet algorithm to approximately halve computation time. To ensure stability, the second-order Verlet method is replaced by a first-order Verlet method for a single time step every 40 time steps so that the decoupled second-order Verlet method does not render the scheme unstable.

2.1. Viscosity

The viscosity term (Eq. (5)) in the equation of motion was originally used to represent both viscosity and prevent particles from interpenetrating. For flows with a free surface, it also has the effect of keeping the scheme stable numerically. However, in many cases, it is too dissipative and affects the shear in the fluid. This is particularly important when using SPH to capture coherent turbulent structures. For viscous fluids, Morris et al. (1997) provided a discretisation of viscosity that was more accurate for low Reynolds number flows. At JHU, we have replaced the standard SPH viscous formulation by introducing a sub-particle scaling technique (Rogers and Dalrymple, 2004) using the Large Eddy Simulation method (LES) approach, similar to that used in incompressible flows (Meneveau and Katz, 2000). For particle methods, Gotoh et al. (2001) use sub-grid scaling for their incompressible MPS method, as do Lo and Shao (2002) for an incompressible SPH method. The basic methodology is that the governing equations are spatially averaged over a length scale comparable to the computation elements. For large-scale eddies, resolved by the grid or particle sizes, the averaged equations are sufficient to solve for these. For the smaller turbulent eddies, smaller than the particle size, a closure scheme is needed to model their effects on the flow field.

Sub-particle scaling (SPS) for a compressible fluid requires a special averaging methodology: we use Favre-averaging ($\tilde{f} = \overline{\rho f}/\bar{\rho}$), which has the advantage of not introducing new terms into the conservation of mass equation (where: $\bar{-}$ denotes an arbitrary spatial filtering). Applying a flat-top spatial filter to the governing equations yields (Yoshizawa, 1986):

$$\frac{d\bar{\rho}}{dt} = -\bar{\rho} \nabla \cdot \tilde{\mathbf{u}} \tag{8}$$

$$\frac{d\tilde{\mathbf{u}}}{dt} = -\frac{1}{\bar{\rho}} \nabla \bar{p} + \mathbf{g} + \frac{1}{\bar{\rho}} (\nabla \cdot \overline{\rho \nu_o} \nabla) \tilde{\mathbf{u}} + \frac{1}{\bar{\rho}} \nabla \cdot \tau^* \tag{9}$$

where τ^* is the sub-particle scale (SPS) stress tensor with elements (in tensor notation):

$$\tau^*_{i,j} = \bar{\rho}\left(2v_t\tilde{S}_{ij} - \frac{2}{3}\tilde{S}_{kk}\delta_{ij}\right) - \frac{2}{3}\bar{\rho}C_I\Delta^2\delta_{ij}. \tag{10}$$

We take C_I to be 0.00066, following Blinn et al. (2002). The Favre-filtered rate of strain tensor is

$$\tilde{S}_{ij} = -\frac{1}{2}\left(\frac{\partial \tilde{u}_i}{\partial x_j} + \frac{\partial \tilde{u}_j}{\partial x_i}\right) \tag{11}$$

We use the standard Smagorinsky model (Smagorinsky, 1963) to determine the eddy viscosity:

$$v_t = (C_s\Delta)^2|\bar{S}|, \tag{12}$$

where the Smagorinsky constant, C_s=0.12, Δ is the initial particle spacing and the local strain rate is given by $|\bar{S}|=(2\bar{S}_{ij}\bar{S}_{ij})^{1/2}$. The sub-particle-scale stresses are discretized using the symmetric formulation of Lo and Shao (2002):

$$\frac{1}{\rho}\nabla\cdot\tau^*|_i = \sum_j m_j\left(\frac{\tau^*_i}{\rho_i^2} + \frac{\tau^*_j}{\rho_j^2}\right)\cdot\nabla_i W_{ij}. \tag{13}$$

2.2. Shephard filtering

When using the LES description of viscous effects in slightly compressible SPH, the application of this methodology can lead to unphysical behaviour at the free surface due to slight density variations being magnified by the equation of state. With the artificial viscosity approach of Monaghan (1992) such variations are damped out, but when using SPS, this can lead to unphysical bumpy surfaces. Colagrossi and Landrini (2003) and Panizzo (2004) showed that, just as the local velocities are averaged in the XSPH term (Eq. (6)), the averaging of the densities helps ensure that the free surfaces are smooth and physically acceptable. We currently perform this filtering every 40 time steps by reinitialising the density of each water particle according to:

$$\rho_i = \frac{\sum_j \rho_j W_{ij} V_j}{\sum_j W_{ij} V_j}. \tag{14}$$

Even with the filtering operations detailed here, the nonlinearities of the physics are still captured by the SPH scheme since the governing equations are not linearised before being expressed in particle form using the SPH formalism. The filtering operations described above, are only conducted within the local region around each particle, and as shown in the results in the following section, allow the numerical method to capture highly nonlinear hydrodynamic processes such as overturning wave fronts, wave impact and splash-up.

3. Examples

3.1. Green water overtopping

Waves overtopping a ship or offshore platform deck can cause immense damage, e.g. Buchner (1996a,b). An unbroken overtopping wave is referred to as 'greenwater.' Trulsen et al. (2002) have developed an irrotational model to examine overtopping, but it is clear that a model should include vorticity and conveniently model flow separation to be successful.

Gomez-Gesteira et al. (2005) used a two-dimensional SPH scheme to examine the overtopping of a flat plate, following the experiments of Cox and Ortega (2002). Fig. 1

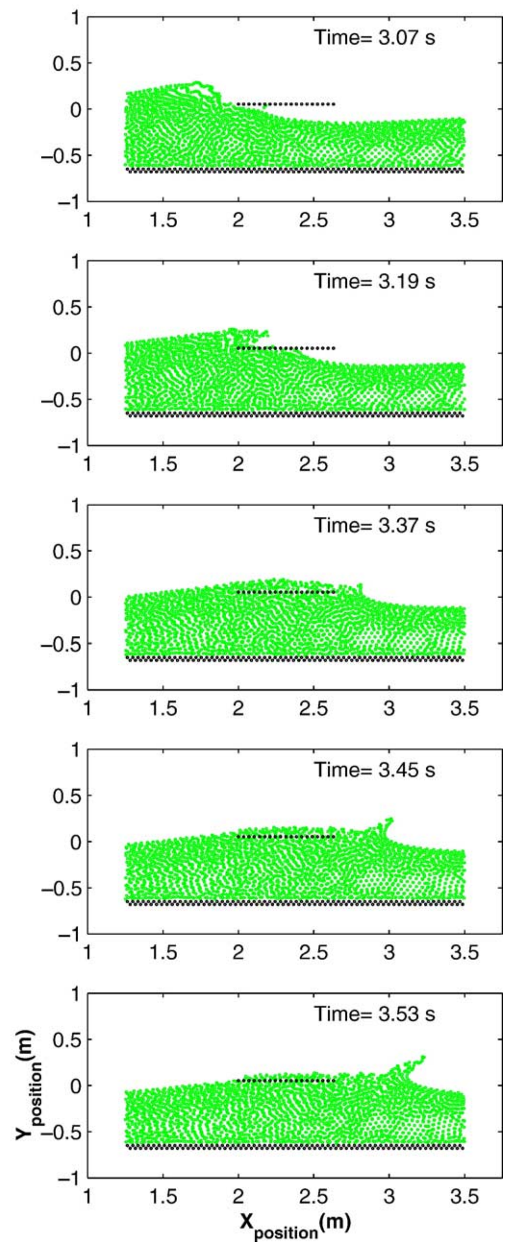

Fig. 1. Time history of overtopping of a flat plate by incident wave from the left. Dots show the position of the SPH particles with time.

shows a large wave impinging on a horizontal plate. The no-flow boundary condition is modelled by using water particles fixed in space that effectively act as solid particles within the scheme (Gomez-Gesteira and Dalrymple, 2004). The wave crest is forced to travel over the top of the plate. Note that the flows under and over the deck recombine at the back of the platform, creating a 'rooster tail.'

3.2. Waves on a beach

The breaking of a wave on a beach is a complicated turbulent process with a number of coherent turbulent structures embedded in the fluid. Nadaoka et al. (1989) discuss obliquely descending eddies, which appear to descend from the bubble cloud left behind by breaking waves. Downbursting, described by Kubo and Sunamura (2001), is a large downrush

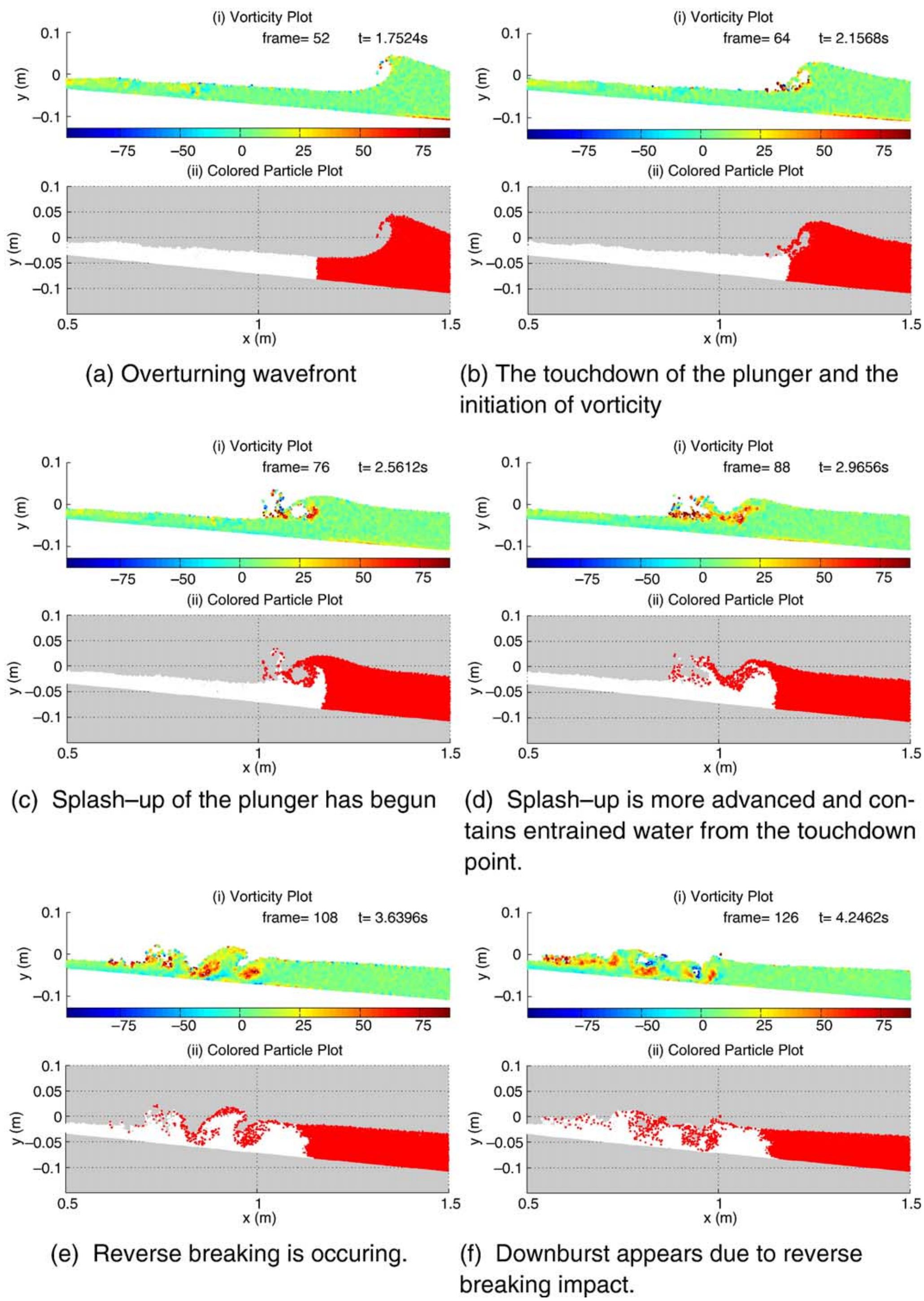

Fig. 2. Weakly plunging breaking wave on a sloping beach. In each subplot, top panel shows particle vorticity, and the bottom panel shows the position of marked offshore water particles.

of water within the water column that impinges on the bed. They idealize this downbursting as due to reverse breaking of the incident wave driving fluid towards the bottom. Finally, there are the presence of wave fingers (or the ropy-looking apparently vortex structures on the backs of some breaking waves that resemble the backs of your fingers as you type, Narayanaswamy and Dalrymple (2002)).

Obliquely descending eddies have been observed in numerical models by Christensen and Deigaard (2001) and Watanabe and Saeki (1999). The SPH model at JHU is currently being used to examine these phenomena with the intent of examining the mechanisms that drives these flows, Section 3.3.2.

Here, in Fig. 2, a sequence of 2-D results presented by Rogers and Dalrymple (2004) are shown for a breaking wave on a beach of slope 1 : 13.5 with an offshore wave height of 0.08 m and a period of 1.4 s. The wave is created by a paddle and breaks as a weakly plunging breaker. In all, 97,915 particles were used in the simulation.

In each part of Fig. 2, the top panel of the figure is a plot of each of the particles colored with its associated vorticity, and the bottom panel displays the fluid divided into two regions colored to show which particles are associated with the plunger (dark) and which are associated with the fluid in front of the wave (light). The vorticity of each particle is defined as (Monaghan, 1992):

$$\omega_i = \sum_j m_j \left(\mathbf{u}_i - \mathbf{u}_j \right) \times \nabla_i W_{ij}. \tag{15}$$

Throughout the process of breaking, several important features are visible: the formation of the plunger, the initiation of the vorticity, the splash-up of the plunger, the reverse breaking that occurs, and the creation of a downburst by the reverse breaker pounding the vortex generated by the initial breaking into the bottom—this is the same mechanism for downbursting as described by Kubo and Sunamura (2001). While reverse breaking might appear unusual, a dramatic example is shown in the solitary wave breaking experiments of Li and Raichlen (2003).

One aspect of the compressibility of the fluid in the SPH model is that there are sound waves within the fluid domain. While the speed of sound has been slowed in the model, the generation of acoustic-like waves by breaking waves still occurs. Fig. 3 shows the time history of fluid pressure as measured by at a point within the surf zone. Three breaking events are clearly shown. The wave train was the same wave and beach as used in the previous simulation, except that three waves propagate through the domain.

3.3. Three-dimensional modeling

The formulation of SPH permits easy extension from two to three dimensions. Here are two examples of three-dimensional SPH applications.

3.3.1. Dam break and structure

Gomez-Gesteira and Dalrymple (2004) examine the 'bore-in-a-box' problem. A rectangular box contains a fixed structure, resembling a building. The box is fitted with a dam near one end, which retains water. The dam is rapidly removed and the fluid rushes out to strike the building and the back wall. The experiments were conducted by Yeh and Petroff at the University of Washington. A previous comparison to these data with a numerical model was carried out by Raad, using his three-dimensional Eulerian–Lagrangian Marker and Micro Cell method and the data and comparisons are given at http://engr.smu.edu/waves/solid.html.

One of the interesting aspects of the experiments is that the bottom of the box was often wet prior to the dam break. This was due to the difficulty in drying out the box between dam

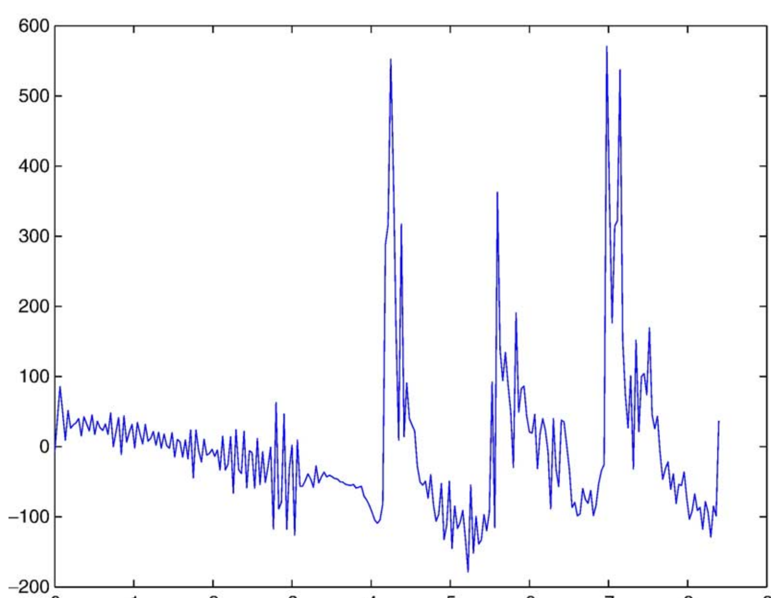

Fig. 3. Time history of pressure (kPa) associated with breaking waves; pressure record at a point in the surf zone. The spikes occur when breaking occurs.

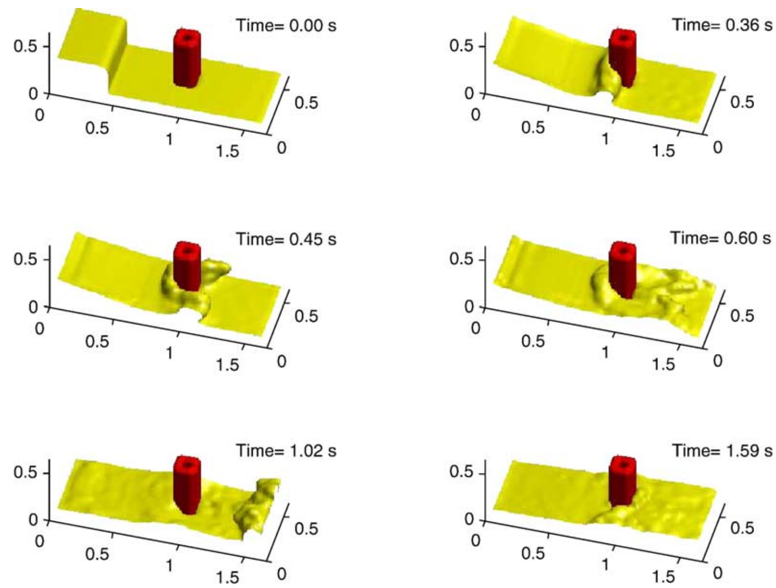

Fig. 4. Time history of the dam break wave in the bore-in-the-box experiment.

break events. The consequences of a wet bed however are significant (see Toro, 2001). While a dry bed dam break behaves like theoretical computations, a wet bed is more complicated as the advancing jet from the dam break pushes up the fluid on the wet bed, forcing it into a backwards moving 'wave.' Fig. 4 shows a time history of the dam break. The number of particles used in the simulation was 35,000, with 15,000 of them being used to form the fixed boundaries.

3.3.2. Waves on a beach

Extending the method in Section 3.3 into three dimensions following Gomez-Gesteira and Dalrymple (2004) and then applying it to the same breaking waves on a beach gives us the results in Fig. 5. The resolution in 3-D is about half that in 2-D unfortunately.

One of the interesting features of the 3-D results is the occurrence of vertical vorticity appearing as a pair of counter rotating vortices. These vorticies persist after breaking and appear to behave like obliquely descending eddies. The full confirmation of this conclusion awaits a higher resolution run of the model.

4. Conclusions

The SPH technique, with its Lagrangian formulation, provides a methodology for the detailed examination of water

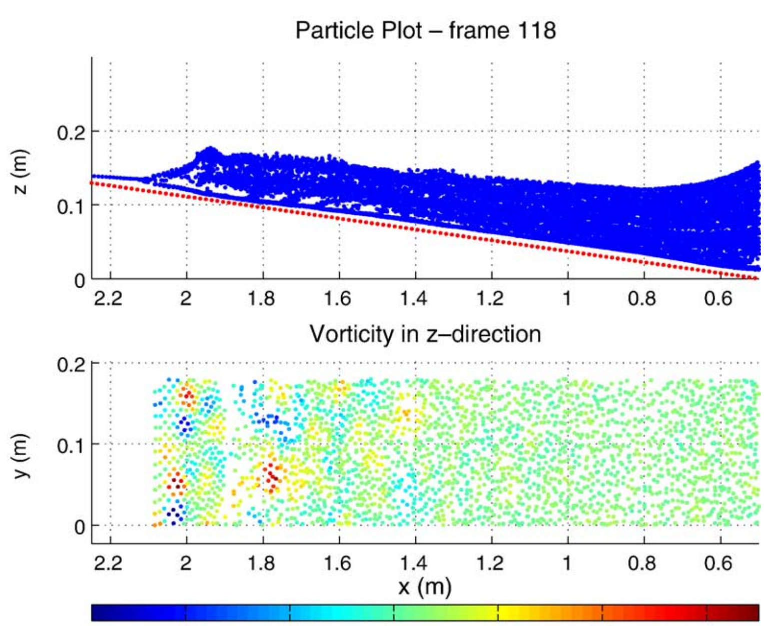

Fig. 5. Three-dimensional weakly breaking wave. Top figure shows the view through the side of the basin. The lower figure shows the vertical component of vorticity, with two counter rotating vorticies located at approximately $x = 1.78$. A wavemaker is located at $x = 0.0$.

waves. It is particularly suited to those cases where there is splash, or flow separation, as the determination of the free surface is not difficult. Improvements conducted at Johns Hopkins such as sub-grid scaling, Shephard filtering, and a new time stepping algorithm are detailed here.

For the examples shown here, realistic results are shown. The development of the JHU SPH model is still ongoing and the results shown are at the 'proof of concept' stage requiring further analysis and detailed comparison with other numerical models and experimental data. For the case of waves breaking on the beach, there are hints that downbursting and obliquely descending eddies have been obtained by SPH. Higher resolution results will soon be able to verify this.

The methodology does require a large number of particles in the simulation for resolution. Further, since the fluid is compressible, there is a sound speed in the model. The result of both of these considerations is that the time steps in the model are dictated by the particle size and the speed of sound so that the time steps are often of O (10^{-5} s). Clearly the method is good for close-up examinations of relatively small regions, where the number of particles can be held to a reasonable number. It is not suitable to model large areas, which are more efficiently modeled by extended Boussinesq codes for example.

Acknowledgments

The authors gratefully acknowledge Office of Naval Research support through grant N00014-04-1-0089. Mr. Shan Zuo provided Fig. 3; thanks, Shan. Also, Dr. Andrea Panizzo (Universita degli Studi di Roma) and Dr. Moncho Gomez Gesteira (University of Vigo) have provided valuable support and assistance for this work.

References

Blinn, L., Hadjadj, A., Vervisch, L., 2002. Large eddy simulation of turbulent flows in reversing systems. In: Vuillermoz, P., Comte, P., Lesieur (Eds.), Selected Proc. of the 1st French Seminar on Turbulence and Space Launchers. CNES, Paris.

Buchner, B., 1996a. The influence of bow shape of FPSOs on drift forces and green water. Proceedings of the Offshore Technology Conference, pp. 389–400. Paper 8073.

Buchner, B., 1996b. The impact of green water on FPSO design. Proceedings of the Offshore Technology Conference, pp. 45–57. Paper 7698.

Chen, G., Kharif, C., Zaleski, S., Li, J., 1999. Two-dimensional Navier–Stokes simulation of breaking waves. Physics of Fluids 11 (1), 121–133.

Christensen, E.D., Deigaard, R., 2001. Large eddy simulation of breaking waves. Coastal Engineering 42, 53–86.

Colagrossi, A., Landrini, M., 2003. Numerical simulation of interfacial flows by smoothed particle hydrodynamics. Journal of Computational Physics 191, 448–475.

Cox, D.T., Ortega, J.A., 2002. Laboratory observations of green water overtopping a fixed deck. Ocean Engineering 29, 1827–1840.

Gomez-Gesteira, M., Dalrymple, R.A., 2004. Using a 3D SPH method for wave impact on a tall structure. Journal of Waterway, Port, Coastal, and Ocean Engineering, Ocean Engineering 130 (2), 63–69.

Gomez-Gesteira, M., Cerquiero, D., Crespo, A.J.C., Dalrymple, R.A., 2005. Green water overtopping analyzed with an SPH model. Ocean Engineering 32 (2), 223–238.

Gotoh, H., Shibihara, T., Sakai, T., 2001. Sub-particle-scale model for the MPS method — Lagrangian flow model for hydraulic engineering. Computational Fluid Dynamics Journal 9 (4), 339–347.

Grilli, S.T., Guyenne, P., Dias, F., 2000. Numerical computation of 3D overturning waves. Proc. 15th Workshop on Water Waves and Floating Bodies. Dan Caesarea, Israel. February 2000.

Koshizuka, S., Nobe, A., Oka, Y., 1998. Numerical analysis of breaking waves using the moving particle semi-implicit method. International Journal of Numerical Methods in Fluids 26, 751–757.

Kubo, H., Sunamura, T., 2001. Large-scale turbulence to facilitate sediment motion under spilling waves. Proceedings, Coastal Dynamics '01, ASCE, pp. 212–221.

Li, Y., Raichlen, F., 2003. Energy balance model for breaking solitary wave runup. Journal of Waterways, Ports, Coastal, and Ocean Engineering, ASCE 129 (2), 47–59.

Lin, P., Liu, P.L.-F., 1998. A numerical study of breaking waves in the surf zone. Journal of Fluid Mechanics 359, 239–264.

Liu, G.R., Liu, M.B., 2003. Smoothed Particle Hydrodynamics: a meshfree particle method. World Scientific. 472 pp.

Lo, E., Shao, S., 2002. Simulation of near-shore solitary wave mechanics by an incompressible SPH method. Applied Ocean Research 24, 275–286.

Meneveau, C., Katz, J., 2000. Scale-invariance and turbulence models for large-eddy simulation. Annual Review of Fluid Mechanics 32, 1–32.

Monaghan, J.J., 1989. On the problem of penetration in particle methods. Journal of Computational Physics 82 (1), 1–15.

Monaghan, J.J., 1992. Smoothed particle hydrodynamics. Annual Review of Astronomy and Astrophysics 30, 543–574.

Monaghan, J.J., 1994. Simulating free surface flows with SPH. Journal of Computational Physics 110, 399–406.

Monaghan, J.J., Kos, A., 1999. Solitary waves on a Cretan beach. Journal of Waterway Port, Coastal and Ocean Engineering 125 (3), 145–154.

Morris, J.P., Fox, P.J., Zhu, Y., 1997. Modeling low Reynolds number incompressible flows using SPH. Journal of Computational Physics 136, 214–226.

Nadaoka, K., Hino, M., Koyano, Y., 1989. Structure of the turbulent flow field under breaking waves in the surf zone. Journal of Fluid Mechanics 204, 359–387.

Narayanaswamy, M., Dalrymple, R.A., 2002. An experimental study of surface instabilities during wave breaking. Proc. 28th Intl. Conference on Coastal Engineering, World Scientific, vol. 1, pp. 344–355.

Panizzo, A., 2004. Physical and numerical modelling of subaerial landslide generated waves, Ph.D. dissertation, Universita Degli Studi di L'Aquila, Italy. 118 pp.

Rogers, B.D., Dalrymple, R.A., 2004. SPH modeling of breaking waves. Proc. 29th Intl. Conference on Coastal Engineering. World Scientific Press, pp. 415–427.

Smagorinsky, J., 1963. General circulation experiments with the primitive equations: I. The basic Experiment. Monthly Weather Review 91, 99–164.

Toro, E.F., 2001. Shock-Capturing Methods for Free-Surface Shallow Flows. John Wiley. 326 pp.

Trulsen, K., Spjelkavik, B., Mehlum, E., 2002. Green water computed with a spline-based collocation method for potential flow. International Journal of Applied Mechanics and Engineering 7 (1), 107–123.

Verlet, L., 1967. Computer "experiments" on classical fluids: I. Thermodynamical properties of Lennard–Jones molecules. Physical Review 159, 98–103.

Watanabe, Y., Saeki, H., 1999. Three-dimensional large eddy simulation of breaking waves. Coastal Engineering Journal 41 (3–4), 281–301.

Wu, T.R., 2004. A numerical study of breaking waves and turbulence effects, Ph.D. Thesis, Cornell University.

Yoshizawa, A., 1986. Statistical theory for compressible turbulent shear flows, with application to subgrid modeling. Physics of Fluids A 29, 2152–2164.